16th World Conference on Earthquake, 16WCEE 2017

Santiago Chile, January 9th to 13th 2017

Paper N° 1526

Registration Code: S-C1461912182

AN ALTERNATIVE SEISMIC HAZARD DEFINITION FOR STRUCTURES SENSITIVE TO BI-DIRECTIONAL EARTHQUAKE EXCITATION

C. I. Nievas[(1)], T. J. Sullivan[(2)]

[(1)] *PhD candidate, ROSE Programme, UME School, IUSS Pavia, Italy, cecilia.nievas@umeschool.it*
[(2)] *Associate Professor, Dept. of Civil and Natural Resources Engineering, University of Canterbury, New Zealand, timothy.sullivan@canterbury.ac.nz*

Abstract

Although earthquake ground motions are complex three-dimensional phenomena, the seismic design of a structure is usually carried out considering horizontal ground shaking in two perpendicular directions only. While the issue of ground motion dependence on the orientation of the recording devices has been the focus of many significant developments during the last decade, the effects of directionality on the characteristics of the structure has received less attention. This paper uses three case-study structural typologies and a set of 405 ground motion pairs from the Reference Database for Seismic Ground-Motion in Europe (RESORCE) to demonstrate the relevance of accounting for directionality in the design and assessment of structures. An alternative definition of hazard that breaks down the problem into an orientation-independent and an orientation-dependent component is proposed with the aim of achieving uniformity in the likelihood of different types of buildings exceeding a certain limit state. The challenges associated with the incorporation of this new perspective to seismic codes within the context of Performance-Based Earthquake Engineering are discussed. Though the focus of this work is set on elastic response of single-degree-of-freedom (SDOF) systems, the approach presented herein is considered to be a fundamental initial step towards a design philosophy that guarantees that the seismic performance of a building does not depend on its sensitivity to the angle of incidence of ground motions.

Keywords: directionality; strong motion; performance-based earthquake engineering; probabilistic assessment.

1. Introduction

Earthquake ground motions are complex three-dimensional phenomena, yet the seismic design of a structure is usually carried out considering horizontal ground shaking in two perpendicular directions. For many decades, little thought appears to have been given to the inherent complexity of the problem, and the two directions considered were those of the recording device, for the case of the ground motions themselves, and those to which most of the structural elements of a building are aligned, for the case of the structures. However, the demand that a particular ground motion imposes on a structure can vary significantly at different orientations [*e.g.* 1, 2, 3].

The issue of *directionality*, that is, the combined effect of the characteristics of ground motions along all possible orientations and their influence on the response of civil engineering structures, comprises two main aspects. The characterisation of ground motions to account for the variation of seismic demand at different directions is the one that has received the most attention in the last two decades. Several orientation-independent definitions of horizontal components of ground motion have arisen in the last 10 years, such as the X^{th} percentile rotationally-dependent geometric mean (GMRotDX [4]) or the X^{th} percentile rotationally-independent component (RotIX [5]). These definitions are computed by rotating each pair of records around all possible non-redundant angles and identifying the demand corresponding to a pre-established percentile X. Yet, despite the evident improvement that this represents over the consideration of ground motions only in their as-recorded directions, information regarding demands at all other orientations is still lost.

The second aspect of the issue of the angle of incidence of ground motions is related to the structures themselves. Even if subject to the same accelerogram pairs, different structural typologies will undergo different demand levels, as a consequence of the dependence of their dynamic properties on directionality. As [3] and [6] point out, there are *azimuth-independent* structures, such as a circular tank, whose response will always be dictated by the largest component of ground motion, because their dynamic properties, as well as their resistance and stiffness, are the same at all possible directions, at least within the elastic range of response. However, most structures are actually *azimuth-dependent* and are subject to the demands that occur along certain directions only. For example, a single-standing rectangular reinforced concrete (RC) wall assumed to be part of a larger system that prevents its out-of-plane displacement is subject to only one component of seismic excitation at a time, and the latter can coincide with the maximum component, the minimum component, or any other in between.

In view of all these issues, this paper illustrates the relevance of accounting for the effects of directionality by means of three structural typologies selected as case-studies. Moreover, an alternative definition of hazard is proposed with the aim of achieving uniformity in the likelihood of different kinds of structures exceeding a certain limit state, building upon the work of Hong and Goda (2007) [1], who suggest that the ratio of the spectral acceleration demand at each angle to the maximum spectral acceleration across all angles, $Sa_{RotD100}$, be used in combination with ground motion prediction equations (GMPEs) to predict the spectral acceleration demand at a given angle. Results obtained from adapting this proposal to the requirements of each building typology are compared with an exact numerical count carried out with a set of 405 ground motions selected from the RESORCE database [7]. Finally, consideration is given to the challenges associated with incorporating this new perspective to seismic codes within the context of Performance-Based Earthquake Engineering.

2. General Concepts

The acceleration at any time *t* at an angle α with respect to the as-recorded direction *x* can be calculated from the as-recorded components $a_{as\text{-}recX}(t)$ and $a_{as\text{-}recY}(t)$ using Eq. (1):

$$a(\alpha, t) = a_{as-recX}(t) \cdot \cos(\alpha) + a_{as-recY}(t) \cdot \sin(\alpha) \quad (1)$$

The direction at which the maximum seismic demand of a ground motion occurs can be considered to be random, both with respect to the source and to the recording device, except when directivity and/or near-fault

effects are of relevance [2]. The direction at which an elastic single-degree-of-freedom (SDOF) oscillator with period T and damping ratio ξ experiences its maximum demand when subject to a particular ground motion is called the *maximum response direction*. For the same ground motion, the maximum response direction varies strongly with the period of the oscillator. The particular values that the maximum acceleration and displacement demands take are referred to as $Sa_{RotD100}(T, \xi)$ and $Sd_{RotD100}(T, \xi)$, respectively [5]. Demands at directions other than that of the maximum response are, by definition, a fraction of the latter, and can thus be represented by a ratio η defined as:

$$\eta(T,\xi,\theta) = Sa(T,\xi,\theta)/Sa_{RotD100}(T,\xi) = Sd(T,\xi,\theta)/Sd_{RotD100}(T,\xi) \quad (2)$$

where θ is the angle with respect to the maximum response direction. Note that $Sd(\theta) = Sd(\theta+180^o)$.

Hong and Goda (2007) [1] studied the statistical behaviour of the ratio η and observed what they called the *goggle phenomenon*: when $\eta(T, \xi, \theta)$ is calculated at all possible directions and represented in a polar plot in which the radius is equal to η in each direction, and the plot is rotated so that its maximum response direction (η=1.00) coincides with the horizontal axis, $\eta(T, \xi, \theta)$ always falls outside two small circles with a radius of 0.50, centred at (0.5,0.0) and (-0.5,0.0), as shown in Fig.1 (top left).

Given that the values that $\eta(T, \xi, \theta)$ can take are bounded by $|\cos(\theta)|$ in the lower end (due to the goggle phenomenon) and 1.00 in the upper end, a generalised beta distribution is highly convenient for characterising its probability of occurrence. The probability density (PDF) of $\eta(T, \xi, \theta)$ can be written as:

$$PDF(\eta) = \frac{(\eta - \beta_{loc})^{\beta_1 - 1} \cdot (\beta_{loc} + \beta_{sc} - \eta)^{\beta_2 - 1}}{B(\beta_1, \beta_2) \cdot \beta_{sc}^{(\beta_1 + \beta_2 - 1)}} \quad (3)$$

where β_1 and β_2 are shape parameters, β_{loc} is the minimum value that $\eta(T, \xi, \theta)$ can take (known as the *location*), β_{sc} is the difference between the maximum and the minimum possible values of $\eta(T, \xi, \theta)$ (known as the *scale*), and B is the Beta function. The probability of observing a value of $\eta(T, \xi, \theta)$ equal to or larger than β_{loc} is equal to 1.00, while the probability of observing a value of $\eta(T, \xi, \theta)$ larger than $\beta_{loc}+\beta_{sc}$ is zero.

Fig.1 shows an example of the distribution of $\eta(T, \xi, \theta)$ at different angles with respect to the direction of maximum response (45º, 60º and 90º, right), and considering all possible orientations together (bottom left), for a subgroup of 324 records from the RESORCE database [7] with epicentral distances between 20 and 25 km, and an oscillator period of 1.0 second. In order to determine the probability distribution of $\eta(T, \xi, \theta)$, a large database of records needs to be used, and the spectral displacement demand of each record at each possible angle needs to be calculated using a small angle increment, to then calculate the corresponding values of η. Records should be grouped so as to be able to assess the possible dependency of $\eta(T, \xi, \theta)$ on parameters such as earthquake magnitude, epicentral distance, pulse-like characteristics of the records, seismic intensity or geotechnical conditions. A beta distribution (Eq. (3)) can finally be fitted to the histograms of η.

A direct conclusion from the work of Hong and Goda (2007) [1] is that the problem of directionality-dependent seismic demands can be broken down into an orientation-independent and an orientation-dependent component. The first would be the determination of the probability of observing a certain value of peak demand, that is, $Sd_{RotD100}(T, \xi)$, while the second would be the characterisation of the probability distribution of the ratio $\eta(T, \xi, \theta)$ at all possible orientations.

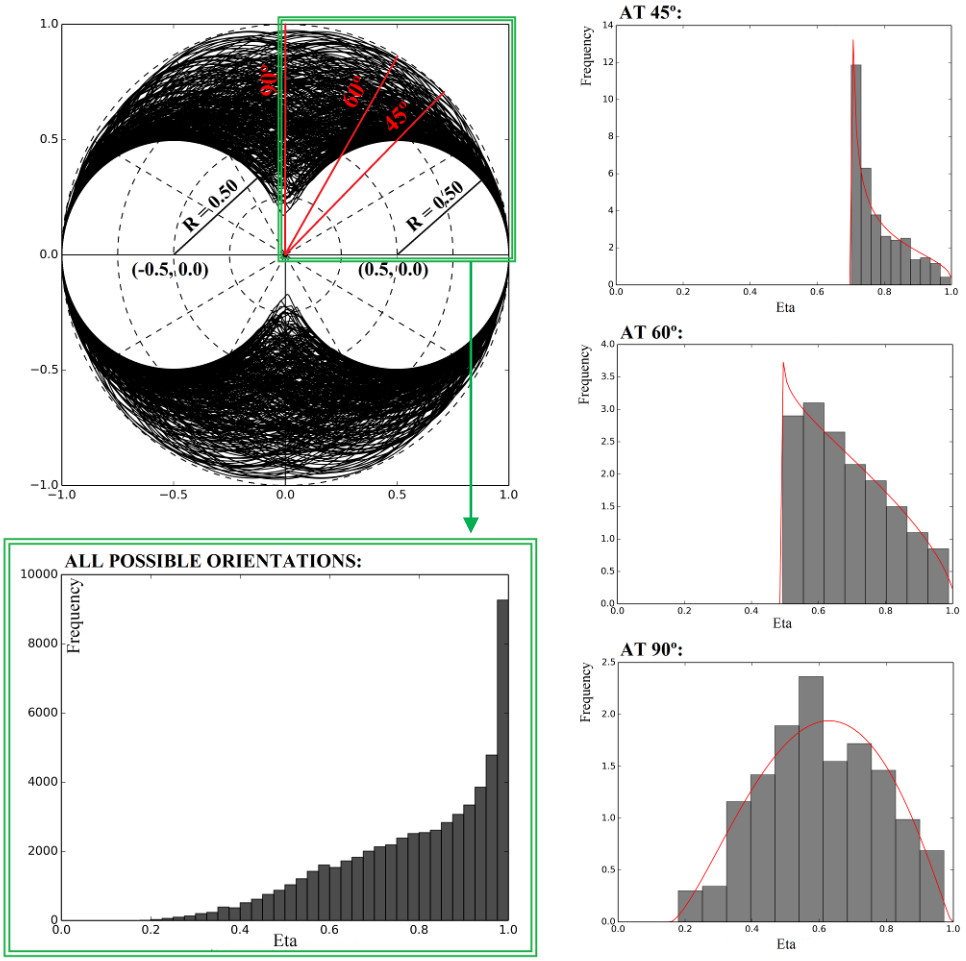

Fig. 1 – Examples of the distribution of the peak displacement ratio $\eta(T, \xi, \theta)$ for T=1.0 s and ξ=5%, using 324 records: polar plot in which the horizontal axis is the direction of maximum response (top left), frequency histograms of $\eta(T, \xi, \theta)$ at specific orientations θ (right), together with corresponding fitted distributions (red lines), and frequency histogram of $\eta(T, \xi, \theta)$ considering all possible orientations (bottom left).

3. Sensitivity of Different Structural Typologies to Directionality

In order to illustrate the relevance of considering the sensitivity of different building typologies to the angle of incidence of ground motions, three case study structures are taken into consideration: (a) an empty circular tank, (b) a building with a rectangular plan, independent lateral resisting systems but the same dynamic properties in two perpendicular horizontal directions, and (c) a reinforced concrete (RC) wall assumed to be part of a larger system that prevents out-of-plane behaviour of the wall to be of relevance (Fig.2). Three different fundamental elastic periods will be considered (0.6, 1.2 and 3.2 seconds), assuming in each case that mass, stiffness and period are the same for the three structures, and that a SDOF system can serve to represent motion in each direction. It is also assumed that these structures behave elastically when subject to the ground motions considered herein. A 5% damping ratio is used throughout this study.

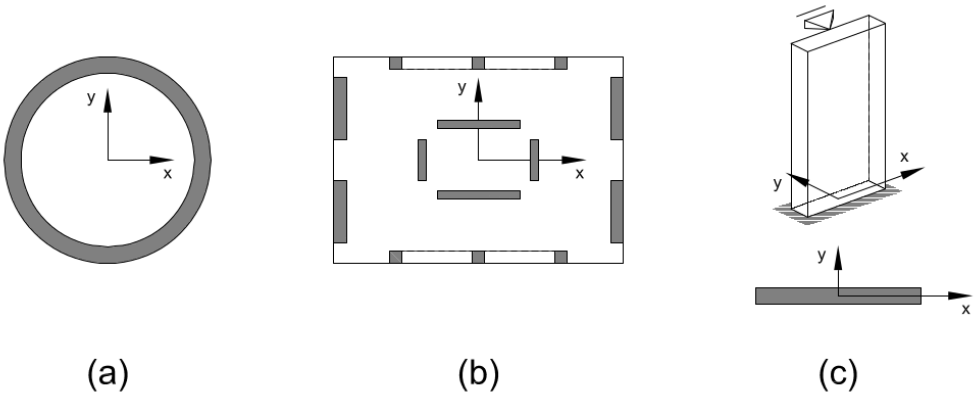

Fig. 2 – Case study structures considered

The existence of an imaginary site for which the seismic hazard is completely defined by a specific set of unscaled real accelerograms is assumed herein to provide a pseudo-deterministic context that allows for the effects of directionality over the exceedance of limit state elastic displacements to be easily identifiable. A group of 405 ground motion pairs has been selected for this purpose from the RESORCE database [7], with magnitudes Mw between 4.0 and 6.0, epicentral distances shorter than 50.0 km, soil type B [8] at the recording site, and a maximum usable period equal to or larger than 3.2 seconds.

Each of the three structures, with each of its three possible periods, is subject to these 405 ground motions at all non-redundant angles rotated every 1°, representing the equal probability of the ground motions being applied in any direction. The exceedance of four different limit states, represented by the displacement of the SDOF systems, is computed for each case. For the case of the circular tank, a limit state displacement is considered as exceeded if exceeded in at least one direction around 360º, for the reasons discussed earlier. For the case of the rectangular building, it is assumed that the exceedance of a limit state displacement at least in one of the two main directions of the building (X,Y) results in the exceedance of the limit state of the system as a whole. Finally, for the case of the RC wall each orientation is considered independently of the rest.

Results are shown in Table 1 through Table 3, for each fundamental period. As expected, the circular tank always presents higher proportions of exceedance than the other two structures, and the RC wall has the lowest proportions of exceedance of the three. If these three case-studies were to be designed according to current codes, the spectral displacement demand would be the same for all structures sharing the same oscillator period (assuming complete dominance of first mode response). The main consequence of this would be that, although having seemingly equal translational dynamic properties, their seismic performance would be different, and the circular tank would be more vulnerable than the rectangular building, which would be, in turn, more vulnerable than the RC wall, simply because of their sensitivity to the angle of incidence of ground motion.

Table 1 – Proportion of cases in which each limit state is exceeded by each case-study structure, for T=0.6 s, calculated by direct exact count from the 405 records and analytically.

Limit State	**max Δ (cm)**	**Count from Time-History Analyses**			**Analytical Approach**		
		Circ. Tank	**Rectangular**	**RC Wall**	**Circ. Tank**	**Rectangular**	**RC Wall**
LS 1	**0.87**	23.21%	20.97%	16.91%	23.21%	21.21%	17.82%
LS 2	**1.73**	9.38%	8.29%	5.90%	9.38%	8.27%	6.55%
LS 3	**3.47**	2.72%	2.23%	1.59%	2.72%	2.34%	1.71%
LS 4	**5.20**	0.99%	0.78%	0.42%	0.99%	0.81%	0.54%

Table 2 – Proportion of cases in which each limit state is exceeded by each case-study structure, for T=1.2 s, calculated by direct exact count from the 405 records and analytically.

Limit State	max Δ (cm)	Count from Time-History Analyses			Analytical Approach		
		Circ. Tank	Rectangular	RC Wall	Circ. Tank	Rectangular	RC Wall
LS 1	**0.87**	27.65%	25.90%	22.55%	27.65%	25.98%	22.83%
LS 2	**1.73**	16.05%	14.41%	11.18%	16.05%	14.43%	11.63%
LS 3	**3.47**	5.19%	4.82%	3.54%	5.19%	4.71%	3.88%
LS 4	**5.20**	3.70%	2.69%	1.70%	3.70%	2.80%	1.96%

Table 3 – Proportion of cases in which each limit state is exceeded by each case-study structure, for T=3.2 s, calculated by direct exact count from the 405 records and analytically.

Limit State	max Δ (cm)	Count from Time-History Analyses			Analytical Approach		
		Circ. Tank	Rectangular	RC Wall	Circ. Tank	Rectangular	RC Wall
LS 1	**0.87**	32.35%	30.73%	26.47%	32.35%	30.58%	26.60%
LS 2	**1.73**	17.53%	16.09%	13.26%	17.53%	16.09%	13.86%
LS 3	**3.47**	8.89%	8.08%	5.68%	8.89%	8.03%	6.24%
LS 4	**5.20**	4.20%	3.53%	2.64%	4.20%	3.61%	2.89%

Fig.3 further illustrates these findings by means of two records selected from amongst the 405. The blue line corresponds to a record from the Mw 5.2 Ierissos (Greece) earthquake of 26th August 1983, while the red line corresponds to Mw 4.4 Marano (Italy) earthquake of 20th February 1980. In both cases the epicentral distance is less than 10.0 km. The figure on the left uses the as-recorded X direction as the horizontal axis, while the figure on the right uses the maximum response direction of each record for T=3.2s instead. The maximum displacement demand at all possible angles ($Sd_{RotD100}$) for a 3.2s oscillator is very similar for both records: 5.579 cm and 5.598 cm for the first and second case, respectively. However, the demand at 90º with respect to the maximum for the Ierissos record is around half of that for Marano (Fig.3, right). Moreover, the directions of maximum response of each record do not occur at the same angle with respect to the as-recorded directions. Due to all this, when these two records are applied to the three case-study structures, the circular tank is subject to (almost) the same maximum displacement in both cases, while the demands for the other two structures are strongly dependent on the direction of application. Table 4 exemplifies this using the largest limit state of the four considered (LS 4, 5.20 cm). At the directions of maximum demand and its perpendicular, the rectangular building exceeds the limit state in one direction for both records, while the limit state is exceeded under just one of the records in the as-recorded directions. An RC wall oriented along the as-recorded X direction would not exceed the limit state in any of the two cases, while it would exceed it for one record were it oriented along the as-recorded Y direction instead. If oriented along the direction of maximum demand, it would be exceeded in both cases, while if oriented along the perpendicular to the latter, it would not be exceeded at all. Finally, if the records were applied at 36º/126º from their as-recorded directions, neither the rectangular building nor the RC wall would exceed the limit state (values close to 5.20 are slightly smaller), while the circular building would still be subject to the same 5.579 cm and 5.598 cm displacement demands. This comparison not only shows the relevance of the angles of incidence, but also how different the demands imposed on structures by two records can be, even if the value of a certain intensity measure of the two is the same, due to the loss of information regarding demands along other directions.

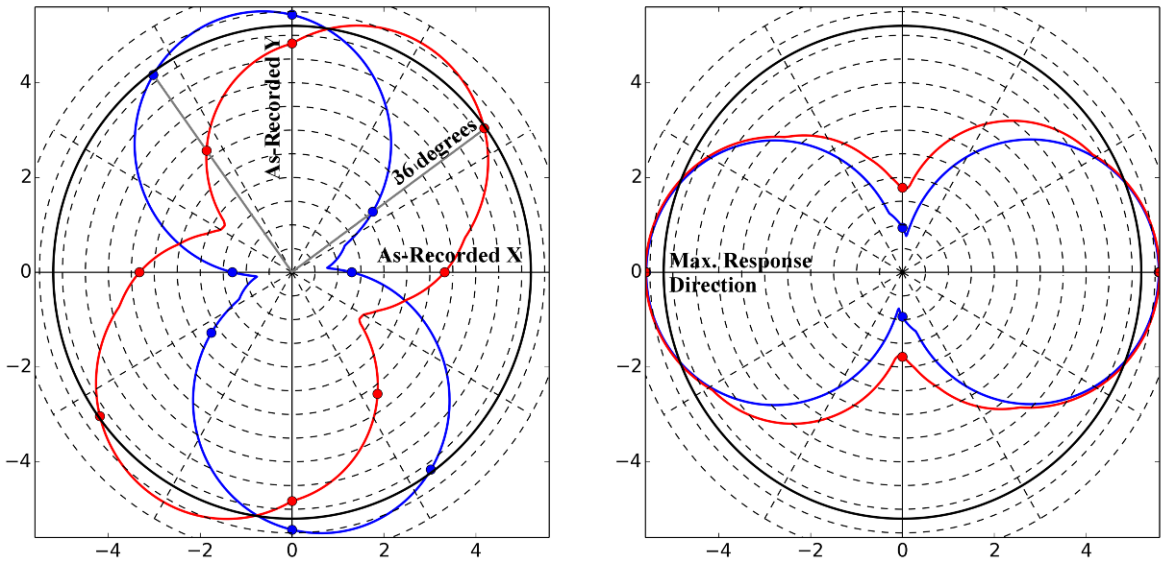

Fig. 3 – Polar plots of elastic spectral displacements (in cm, T = 3.2 s, 5% damping ratio) at all possible angles for two selected records (Ierissos, blue, Marano, red), with the horizontal axis corresponding to the as-recorded X direction (left) and the maximum demand direction (right). The thick-line circle shows the 5.2 cm limit state.

Table 4 – Exceedance of LS 4 (5.20 cm) by each of the case-study structures (T = 3.2 s) when two selected records are applied at certain angles of incidence.

Orientation	Record	Circ. Tank	Rectangular	RC Wall X	RC Wall Y
As-Recorded	Ierissos	yes	yes	no	yes
	Marano	yes	no	no	no
Max. Demand	Ierissos	yes	yes	yes	no
	Marano	yes	yes	yes	no
36° from As-Recorded	Ierissos	yes	no	no	no
	Marano	yes	no	no	no

4. Analytical Framework

The idea of Hong and Goda (2007) [1] of decomposing the problem of seismic demands at different angles of incidence is a highly valuable tool for the consideration of directionality in the design and assessment of structures. While [1] mainly studied the distribution of $\eta(T, \xi, \theta)$ considering a certain orientation θ at a time, it is also possible to determine the probability of $\eta(T, \xi)$ having a certain value at some angle, gathering the information at all possible orientations θ under one single distribution. The former approach can be useful, for example, if one assumes that the maximum response direction coincides with the X axis of the rectangular building (Fig.2b) and wants to know the probability of the demand along the Y axis exceeding a certain percentage of the demand at X. However, if one is interested in knowing the chances of the demand along either X or Y of the rectangular building exceeding a certain percentage of the maximum rotational demand ($Sd_{RotD100}(T, \xi)$) without any knowledge on how the maximum response direction compares to the orientation of the building, the second approach can be of more interest, as it aims at answering the question "*What is the probability of $\eta(T, \xi)$ being equal to a certain value at a random direction, if all angles of incidence of the excitation demand are equally likely?*". Note that $\eta(T, \xi)$ is used here to indicate that all possible angles are

assigned the same probability of occurrence and are considered altogether, as opposed to $\eta(T, \xi, \theta)$, which indicates that η is being considered at one specific angle (θ).

If a record has a certain value of $Sd_{RotD100}(T, \xi)$, it is possible to calculate the probability of it causing a limit state displacement Sd* to be exceeded as the probability of $\eta(T, \xi)$ being equal to or larger than the ratio $Sd^*/Sd_{RotD100}(T, \xi)$. It is then possible to incorporate in this calculation the probability of $Sd_{RotD100}(T, \xi)$ occurring in the first place, and to take into consideration all possible (relevant) values of $Sd_{RotD100}(T, \xi)$ at a site. The total probability of exceedance of Sd* at any direction can be finally written as:

$$P[Sd(T,\xi) \geq Sd^*] = \sum_i P[\eta_i(T,\xi) \geq Sd^*/Sd_{RotD100\,i}(T,\xi) | Sd_{RotD100\,i}(T,\xi)] \cdot P[Sd_{RotD100\,i}(T,\xi)] \quad (4)$$

In continuous form, this equation becomes an integral across the whole of the hazard curve HC(*x*):

$$P[Sd(T,\xi) \geq Sd^*] = \int P\left[\eta_i(T,\xi) \geq \frac{Sd^*}{x}\right] \cdot \left|\frac{dHC(x)}{dx}\right| \cdot dx \quad (5)$$

where *x* is used for clarity to represent $Sd_{RotD100}(T, \xi)$. Assuming that HC(x) is defined in terms of probabilities of exceedance of a given level of ground motion within a specified period of time, the product of the absolute value of the derivative of the hazard curve and *dx* is equal to the probability of $Sd_{RotD100}(T, \xi)$ taking on a specific value of *x* in that time. In practice, this integration will be carried out numerically.

Until now, the probability of $\eta(T, \xi)$ has only been considered in terms of the capacity of ground motions to generate a certain range of spectral demands at different orientations. However, the full benefit of using $\eta(T, \xi)$ will occur when it is used to represent the proportion of $Sd_{RotD100}(T, \xi)$ that a structure is subject to, rather than the proportion of $Sd_{RotD100}(T, \xi)$ that a ground motion can generate. From the structural point of view, the relevant question is not whether Sd* can be exceeded in any possible direction, but whether Sd* can be exceeded for a particular structure. For the RC wall studied above (Fig.2c), if a certain ground motion causes a limit state displacement Sd* to be exceeded only in the direction perpendicular to the plane of the wall, the RC wall will not exceed this limit state (under the assumptions described earlier). Similarly, the rectangular building (Fig.2b) will exceed the limit state defined by Sd* only if the displacement demands in X and/or Y exceed this value. In the case of the RC wall, the minimum possible value of $\eta(T, \xi)$ at an unknown direction is zero, while for the case of the rectangular building it is equal to $\cos(45º) \approx 0.707$, due to the goggle phenomenon. For the circular tank (Fig.2a), $\eta(T, \xi)$ can only take a value of 1.00, because the structure will always experience $Sd_{RotD100}(T, \xi)$ at some relevant direction. Clearly, a beta distribution cannot be fitted to this case, and Eq. (4) simply reduces to:

$$P[Sd(T,\xi) \geq Sd^*] = P[Sd_{RotD100}(T,\xi) \geq Sd^*] \quad (6)$$

As shown in [9], a closer observation of the hazard curves allows for some insight on the contribution of different ground motion levels to the overall probability of exceedance of a certain limit state. If the value of $Sd_{RotD100}(T, \xi)$ of a particular record is smaller than the limit state displacement of interest, Sd*, said record cannot cause the exceedance of Sd* at any angle. As a consequence, all values of $Sd_{RotD100}(T, \xi)$ smaller than Sd* can be directly excluded from the computation. On the other extreme, if $Sd_{RotD100}(T, \xi)$ is sufficiently larger than Sd* it is likely that the latter be exceeded at all directions, because $Sd^*/Sd_{RotD100}(T, \xi)$ will be close to zero and the probability of $\eta(T, \xi)$ exceeding zero will be close to 1.00. In between these extremes lie the cases for which Sd* will be exceeded only at some directions, and for which Eq. (4) needs to be fully computed. The answer to the question of how much larger than Sd* need be $Sd_{RotD100}(T, \xi)$ depends on the structural typology under consideration. For the case of the rectangular building it is clear that, as the minimum possible value of $\eta(T, \xi)$ is 0.707, all values of $Sd_{RotD100}(T, \xi)$ larger than Sd*/0.707 will cause Sd* to be exceeded at some

direction. However, the minimum possible value of $\eta(T, \xi)$ is zero in the case of the RC wall and, thus, even the largest value that $Sd_{RotD100}(T, \xi)$ may physically take might not cause the RC wall to exceed Sd*, if the wall is oriented along a direction with a very small value of $\eta(T, \xi)$. In practice, it should be possible to determine a minimum value of $\eta(T, \xi)$ that is worth considering for these kinds of structures, so that the probability of a smaller $\eta(T, \xi)$ becomes so negligible that accuracy is not compromised. It should be noted that the exclusion of all values of $Sd_{RotD100}(T, \xi)$ smaller than Sd* from the computation can be carried out only when elastic displacements are of interest . Further considerations are needed for inelastic behaviour, as inelastic displacements can be equal, larger or smaller than their corresponding elastic demands [10].

5. Comparison of Results

The framework described can now be applied to the same three case-study structures analysed in Section 4 by means of a count of exceedance cases from time-history analyses. As explained before, the group of 405 ground motion pairs is assumed to fully define the hazard at a site, with each pair having the same probability of occurrence as the rest (1/405), and all angles of incidence between the ground motions and the buildings being equally possible as well. "Pseudo-hazard" curves can be developed from the 405 records for the three oscillator periods under consideration, by simply counting how many records have a $Sd_{RotD100}(T, \xi)$ that exceeds a series of predefined values (i.e. discrete points within the horizontal axis, which are herein taken as the $Sd_{RotD100}(T, \xi)$ value of each individual record, to maximise precision), and dividing the counts by the total number of records. This can be mathematically described by means of the Heaviside function $H[\cdot]$ as follows [11]:

$$P[Sd_{RotD100} \geq x] = \frac{1}{405}\sum_{i=1}^{405} H[Sd_{RotD100\,i} - x] \tag{7}$$

The resulting curves are shown in Fig.4. As expected, these curves are not smooth because they are simple counts of exceedances by a finite number of ground motions. Fig.4 also shows the distributions of $\eta(T, \xi)$ obtained from the 405 records in the set. The top row corresponds to a structural typology in which two perpendicular directions have the same dynamic properties, and exceedance of limit states is defined by exceedance in any of these directions, as is the case of the rectangular building considered herein (Fig.2b). In this case, the distribution is fitted to values of η calculated from the envelope of spectral displacement demands at all non-redundant orientations, that is:

$$\eta_{ENV}(T, \xi, \theta) = \frac{MAX[Sd(T, \xi, \theta),\ Sd(T, \xi, \theta + 90^o)]}{Sd_{RotD100}(T, \xi)} \qquad \forall \theta \in [0^o, 90^o) \tag{8}$$

The bottom row of Fig.4 corresponds, instead, to a structural typology for which each individual orientation is of relevance, such as the RC wall assumed herein to have its out-of plane deformation prevented. The distribution is now fitted to values of η calculated for each angle in the interval [0º,180º). A step of 1º is used to define the distributions for both typologies.

The limit states considered are the same as in Section 4. Table 1 through Table 3 show the results obtained together with the previous ones, determined by means of an exact count of exceedance from time-history analyses. For the circular tank, the ratios of exceedance are exactly the same with both approaches because they only depend on the proportion of records that have a value of $Sd_{RotD100}(T, \xi)$ equal to or larger than Sd*, and not on the distribution of $\eta(T, \xi)$. Analytical results for the rectangular building and the RC wall are very close to those of the exact count, though a larger precision seems to have been achieved for the rectangular building. This can be expected from the fitted distributions of $\eta(T, \xi)$ shown in Fig.4, for which it is clear that the fit is better for this structure than for the RC wall. In addition, results from the analytical approach seem more accurate for smaller values of the limit state displacements than for larger ones. This is due to most records within the set

imposing relatively low demands on these structures, as it is shown in Fig.5. Though this characteristic of this set of records is accounted for in the pseudo-hazard curves, i.e. in the probability of a certain value of $Sd_{RotD100}(T, \xi)$ happening, the lack of density in the data related to large demands causes the distribution of $\eta(T, \xi)$ not to be sufficiently sampled when carrying out the exact count of exceedances.

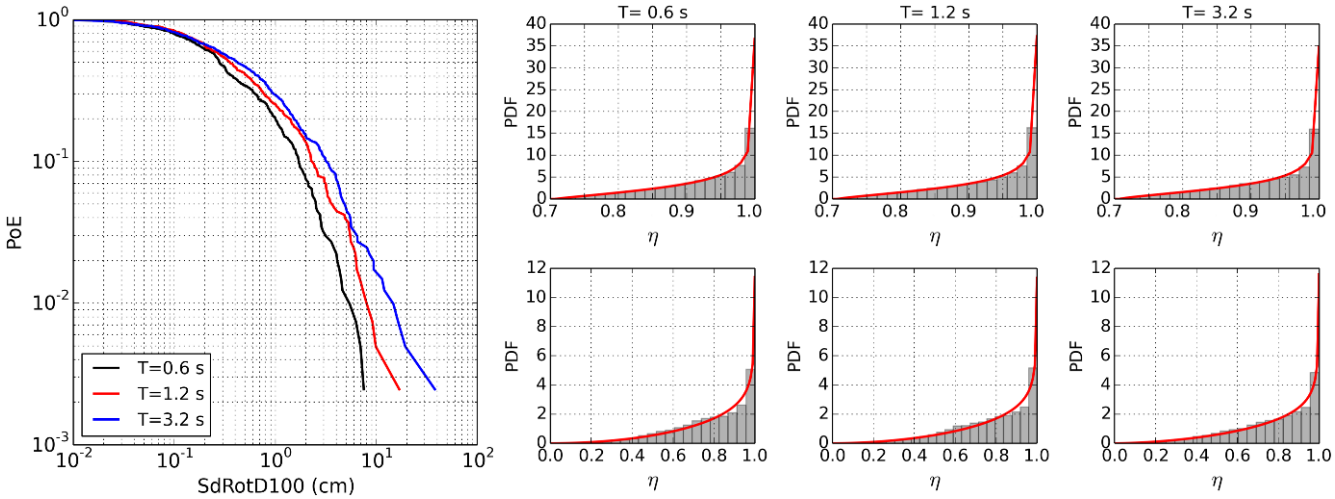

Fig. 4 – Pseudo-hazard curves corresponding to the set of 405 records, in terms of $Sd_{RotD100}$, for three oscillator periods of interest (left), and typology-specific probability density functions (PDF) of $\eta(T, \xi)$ for the rectangular building (right, top row) and the RC wall (right, bottom row), for the same three oscillator periods.

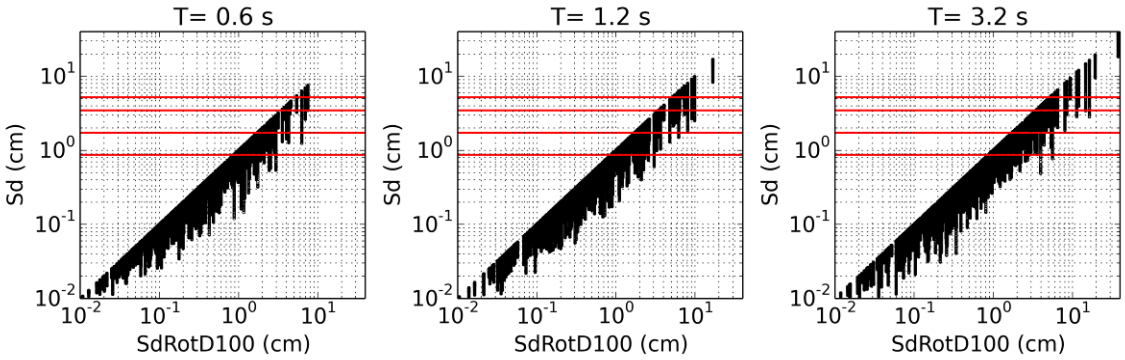

Fig. 5 – Spectral displacement demands at all possible orientations against $Sd_{RotD100}(T, \xi)$ of the 405 records for three oscillator periods of interest. Red horizontal lines indicate the four limit states considered.

6. Towards Uniform-Risk Design

The results and considerations presented above demonstrate a fundamental caveat associated to the design of structures for uniform hazard. While a structure like the circular tank will always be subject to $Sd_{RotD100}(T, \xi)$, the rectangular building and RC wall used in this study will not be exposed to this value unless they are adequately aligned with the direction at which it occurs, and will more likely be subject to smaller demands. This is clearly undesirable from the perspective of Performance-Based Earthquake Engineering, for design under these conditions leads to structures performing differently than what they were intended, due to their sensitivity to directionality. If considered from the perspective of the rectangular building and RC walls being over-designed with respect to the circular building, the effect does not seem as objectionable as it does when the circular building is seen as being under-designed with respect to the other two. However, it is the latter

interpretation that should be embraced, for, when subject to the same ground motion, the rectangular building and RC walls may or may not be subject to $Sd_{RotD100}(T, \xi)$, while the circular tank certainly will. In other words, if all three structures are designed for that particular value of $Sd_{RotD100}(T, \xi)$, the rectangular building and RC walls may or may not be over-designed when subject to it, while the circular tank will undoubtedly be under-designed if designed for less.

With this in mind, the question should now be how to design each type of structure so that their probability of exceeding a specific limit state is the same. For the time being, this reflection will leave aside the additional complications that arise from the consideration of inelastic behaviour and modes of vibration other than the fundamental one, for these are the matter of ongoing research. As a first step, the probability of exceeding a specific limit state should be specified as a target for all structures to comply with. Then, displacement design spectra calculated accounting for directionality could be provided for different structural typologies. These could be determined as shown in Section 4, combining hazard curves defined in terms of $Sd_{RotD100}(T, \xi)$ with the distribution of $\eta(T, \xi)$ appropriate for each typology. A first potential difficulty associated with this approach is related to the impossibility of defining beforehand all possible cases of interest for the practitioner. While this study has dealt with three particular typologies, an infinite number can arise simply from the definition of rectangular buildings with different dynamic properties in their two main structural axes, for example. It would thus be desirable to be able to provide practitioners with the tools needed to calculate the probabilities of exceeding limit states for any structure they may wish. Along this line of thought, the relationships developed by [2, 12] can be useful to determine the correlation between directions of maximum response and magnitude of demands at different periods in two perpendicular directions, and can be easily implemented within the approach presented herein to cover the case of a rectangular building with different dynamic properties in its two main structural axes. A second difficulty may arise from the possible dependency of $\eta(T, \xi)$ on parameters such as moment magnitude, epicentral distance, or others. As $Sd_{RotD100}(T, \xi)$ is calculated by means of a probabilistic seismic hazard analysis, decisions might need to be made with respect to which value of magnitude or distance to consider, if the distribution of $\eta(T, \xi)$ is provided separately from $Sd_{RotD100}(T, \xi)$.

Still focusing on the elastic SDOF case, it would be possible to use one spectral displacement spectrum calculated in terms of $Sd_{RotD100}(T, \xi)$ to determine the properties of an equivalent azimuth-independent structure (like the circular tank herein), and then modify them to account for the desired typology. An azimuth-independent typology would be designed directly to the value of $Sd_{RotD100}(T, \xi)$ equal to the specified limit state displacement Sd*, associated to the specified probability of exceedance (*e.g.* 10% in 50 years). As the displacement demand increases with period (for periods of vibration smaller than the corner period of the displacement spectrum), an azimuth-dependent structure should then be designed to be more flexible (*i.e.* have a longer fundamental period) than the equivalent azimuth-independent structure. The period that causes the azimuth-dependent structure to have the same probability of exceeding Sd* as the latter can be calculated numerically by making Eq. (5) equal to this probability of exceedance and determining the period that satisfies this criterion. This procedure clearly needs iteration, as the terms on the right of the equality in Eq. (5) depend on the structural period themselves. It would perhaps be of interest to generate approximations to the hazard curves and to the distribution of $\eta(T, \xi)$ that would allow for a simplification in this calculation and, hopefully, a closed-form solution of Eq. (5) for a predefined value of the probability of exceedance. Furthermore, future research could aim at developing expressions that allow to calculate the stiffness that the azimuth-dependent structure should have, as a function of that of the equivalent azimuth-independent one.

7. Conclusions

This paper has demonstrated the relevance of accounting for directionality in the design and assessment of different structural typologies by means of three case-study buildings, whose elastic responses to a set of 405 ground motions selected from the RESORCE database [7] were analysed at all possible orientations. Moreover, a new analytical approach, which builds upon the work of Hong and Goda (2007) [1], has been presented, and its effectiveness demonstrated by comparing the probabilities of exceeding a series of pre-defined limit state displacements calculated analytically against an exact numerical count. As the approach breaks down the

problem into an orientation-independent and an orientation-dependent component, a way towards achieving uniformity in the likelihood of different kinds of buildings exceeding a certain limit state is facilitated, as only one of the two components is typology-dependent. Future research should aim at further extending the methodology to incorporate the effects of non-linear response and higher modes of vibration, as well as to developing the best way to incorporate this new perspective to seismic codes within the context of Performance-Based Earthquake Engineering. Though the focus has been set on elastic response of SDOF systems, the approach presented herein is considered to represent a fundamental initial step towards a design philosophy that guarantees that the seismic performance of a building does not depend on its sensitivity to the angle of incidence of ground motions.

8. References

[1] Hong HP, Goda K (2007): Orientation-dependent ground-motion measure for seismic hazard assessment. *Bulletin of the Seismological Society of America*, **97**, 1525–1538.

[2] Shahi SK, Baker JW (2014): NGA-West2 models for ground motion directionality. *Earthquake Spectra*, **30**, 1285–1300.

[3] Grant DN, Padilla D, Greening PD (2011): Orientation dependence of earthquake ground motion and structural response. In: *Protection of Built Environment Against Earthquakes*, pp. 57–73.

[4] Boore DM, Watson-Lamprey J, Abrahamson N (2006): Orientation-independent measures of ground motion. *Bulletin of the Seismological Society of America*, **96**, 1502–1511.

[5] Boore DM (2010): Orientation-independent, nongeometric-mean measures of seismic intensity from two horizontal components of motion. *Bulletin of the Seismological Society of America*, **100**, 1830–1835.

[6] Stewart JP, Abrahamson NA, Atkinson GM, Baker JW, Boore DM, Bozorgnia Y, Campbell KW, Comartin CD, Idriss IM, Lew M, Mehrain M, Moehle JP, Naeim F, Sabol TA (2011): Representation of bidirectional ground motions for design spectra in building codes. *Earthquake Spectra*, **27**, 927–937.

[7] Akkar S, Sandkkaya M, Senyurt M, Azari Sisi A, Ay B, Traversa P, Douglas J, Cotton F, Luzi L, Hernandez B, Godey S (2014): Reference database for seismic ground-motion in Europe (RESORCE). *Bulletin of Earthquake Engineering*, **12**, 311–339.

[8] CEN (2004): *Eurocode 8: Design of Structures for Earthquake Resistance - Part 1: General rules, seismic actions and rules for buildings.* European Committee for Standardization, Brussels, Belgium.

[9] Nievas CI, Sullivan TJ (2016): Accounting for directionality as a function of structural typology in performance-based earthquake engineering design. *Earthquake Engineering and Structural Dynamics*, UNDER REVISION.

[10] FEMA (2005): *Improvement of Nonlinear Static Seismic Analysis Procedures – FEMA 440*. Applied Technology Council (ATC-55) and Department of Homeland Security of the Federal Emergency Management Agency, United States.

[11] Ebel JE, Kafka AL (1999): A Monte Carlo Approach to Seismic Hazard Analysis. *Bulletin of the Seismological Society of America*, **89**, 854-866.

[12] Baker JW, Cornell CA (2006): Correlation of response spectral values for multicomponent ground motions. *Bulletin of the Seismological Society of America*, **96**, 215–227.